Apparent slip at the surface of a ball spinning in a concentrated suspension

By L. A. MONDY[1], A. M. GRILLET[1], G. PACHECO[1]†,
J. HENFLING[1], M. S. INGBER[2], A. L. GRAHAM[3]
AND H. BRENNER[4]

[1]Sandia National Laboratories, Albuquerque NM 87185-0834, USA

[2]Department of Mechanical Engineering, University of New Mexico, Albuquerque NM 87131, USA

[3]Los Alamos National Laboratory, Los Alamos, NM 87545, USA

[4]Department of Chemical Engineering, Massachusetts Institute of Technology, Cambridge MA 02139, USA

The couple on a ball rotating relative to an otherwise quiescent suspension of comparably-sized, neutrally buoyant spheres is studied both experimentally and numerically. Apparent 'slip' relative to the analytical solution for a sphere spinning in a Newtonian fluid (based upon the viscosity of the suspension) is determined in suspensions with volume fractions c ranging from 0.03 to 0.50. This apparent slip results in a decrease of the measured torque on the spinning ball when the radius of the ball becomes comparable with that of the suspended spheres. Over the range of our data, the slip becomes more pronounced as the concentration c increases. At $c = 0.25$, three-dimensional boundary-element simulations agree well with the experimental data. Moreover, at $c = 0.03$, good agreement exists between such calculations and theoretical predictions of rotary slip in dilute suspensions.

1. Introduction

Previous experimental studies (Mondy, Graham & Jensen 1986) exploring a fairly wide range of parameters have shown that the (mean‡) sedimentation velocity of a ball falling under the influence of gravity through an otherwise quiescent suspension of similarly-sized neutrally buoyant particles appears to be the same as would occur in a hypothetical single-phase Newtonian fluid continuum of viscosity μ_s, with no-slip occurring at the surface of the falling ball. Later experimental studies (Milliken *et al.* 1989) yielded results consistent with this, provided that the ball size was not too small relative to that of the suspended particles. In the dilute limit, the experimental results are supported by the theoretical work of Almog & Brenner (1997).

---

† Present address: Honeywell, San Diego, CA 92173, USA.

‡ The instantaneous velocity of the ball varies in time depending upon its momentary proximity to neighbouring particles. As a result, the particle trajectory experiences numerous fluctuations from its mean motion. The mean sedimentation velocity of the falling ball is defined simply as the vertical distance through which it falls divided by the time of fall, in the limit, of 'long times' involving a sufficient number of 'collisions' with the suspended particles to assure that the measured mean velocity is statistically significant. That this mean velocity is an intrinsic property of the fluid–particle/falling-ball system, independent of initial conditions, etc., is a well-established experimental fact. We mention this fact explicitly in order to compare the contrasting behaviour observed in the rotary sphere case discussed in this paper.

Almog & Brenner (1998) have shown, to terms of the first order in the volume fraction c of suspended particles, that the couple L on a ball of radius a_1 rotating at constant angular velocity Ω in an otherwise quiescent unbounded suspension of uniformly-sized spheres of radii a_2 is not that expected from solving the Stokes equations with a stick boundary condition at the ball surface (Stokes 1851; Happel & Brenner 1986), namely

$$L = 8\pi\mu_s a_1^3 \Omega, \qquad (1)$$

until the size ratio a_2/a_1 tends towards zero. Their theory describes the behaviour of dilute suspensions, where μ_s is given by Einstein's (1906, 1911) formula, $\mu_s = \mu_0(1 + 5c/2)$, with μ_0 the viscosity of the pure suspending solvent. If we assume that the suspension as a whole can be represented as a hypothetical single-phase continuum, the diminution in L predicted by Almog & Brenner (1998) can be interpreted as a reduction in the rotational friction factor owing to a partial slip boundary condition acting uniformly over the sphere surface. Such slip models are employed to interpret rotational diffusion measurements of molecular tracers. The Stokes–Einstein–Debye (SED) model (Stokes 1851; Einstein 1956; Debye 1929), which treats the solvent as a hydrodynamic continuum characterized only by a viscosity and temperature, can be surprisingly successful even when being applied on a molecular scale (for example, Ben-Amotz & Scott 1987). Sluch, Somoza & Berg (2002) have shown that the SED rotational relationship with slip boundary conditions can hold, even if the solute molecule is distinctly smaller than the solvent molecules. Koenderink (2003) employed this rationale to model successfully the deviations from short-time, rotational, SED scaling for colloidal hard-sphere suspensions. He described the drag on the rotating tracer 'as the sum of a drag contribution due to the solvent (which sticks) and a drag contribution due to the (hydrodynamic) interactions with the host particles', explaining that there was no reason to suppose that the discrete particle phase would exhibit a stick boundary condition.

To further study the hydrodynamic effects of the presence of suspended particles, we report here experimental measurements of the couple experienced by a spinning ball immersed in a neutrally buoyant suspension of spheres dispersed in a Newtonian liquid in the concentration range $0.20 \leqslant c \leqslant 0.50$. The size ratio a_2/a_1 varied from 0.026 to 1.00. In this size range Almog & Brenner (1998) predict an observable 'slip', one that depends strongly on the size ratio. Such slip is also observed to occur experimentally in our moderate- to high-concentration suspensions. As we decreased the size of the spinning ball relative to the size of the suspended spheres, the apparent spinning-ball viscosity decreased dramatically, thereby the suspension exhibited an apparent 'slip' on the surface of the spinning ball.

Kunesh (1971) (see also Kunesh *et al.* 1985) measured the hydrodynamic resistance to rotation of a ball at small Reynolds number, thereby confirming (1) for the hydrodynamic torque exerted on a sphere submerged in a homogeneous Newtonian liquid. In their experiments, the fluid was contained within a circular cylinder which was rotated at uniform angular velocity Ω on a turntable, while the ball – which was suspended by an overhead torsion wire connected to a fixed platform lying outside of the liquid – remained at rest. In our comparable suspension experiments we, like Kunesh *et al.* (1985), measured the torque on the ball by recording the small angle of deflection of a thin, carefully calibrated torsion wire suspending the ball from a fixed platform, while a cylindrical vessel containing an otherwise quiescent suspension was rotated at a constant angular rate. To confirm the reliability of our system, the viscosity of a suspension-free Newtonian liquid was measured with our 'spinning-ball

rheometer' and found to lie within 1 % to 5 % (depending on ball size and rotation speed) of the viscosity measured in a conventional capillary viscometer. Thus, we were able to obtain viscosity measurements in our home-built viscometer with roughly the same accuracy as that in (much smaller) commercially available torsional viscometers.

As regards terminology, we refer to our apparatus as a 'spinning-ball viscometer', despite the fact that ball itself does not spin (relative to a laboratory-fixed reference frame). Rather, it is the cylinder walls bounding the suspension, and hence the suspension itself, that spins (again in the laboratory frame). Thus, in the absence of the stationary suspended ball, the suspension would simply undergo a rigid-body rotation. From the point of view of low-Reynolds-number hydrodynamics, where centrifugal effects are negligible, it is immaterial whether the ball spins and the cylinder walls are at rest or vice versa. Only the relative ball/wall rotation rate is important. Thus, our description of the apparatus as a 'spinning-ball' device is entirely appropriate. (Indeed, from the point of view of an observer fixed in the cylinder walls, and hence rotating with the suspension, the ball would appear to rotate at the appropriate angular velocity. Of course, we are assuming that the suspension as a whole adheres to the cylinder walls.)

The experimental apparatus allowed us to record the instantaneous time history of the measured couple on the ball during the course of any one experiment (as the particulate configuration of the suspension evolved in time owing to shear-induced particle migration away from the neighbourhood of the ball). As subsequently discussed, the short-time behaviour observed, following start-up, confirms the existence of 'apparent slip', a phenomenon theoretically quantified by Almog & Brenner (1998), albeit only in the case of dilute suspensions. The slip became more pronounced as the concentration of the suspended particles increased. In the more concentrated suspensions, the couple was observed to diminish with time towards an asymptotic limiting value, presumably because the suspended particles moved, on average, away from the ball as a result of 'shear-induced diffusion' effects of the type first identified by Leighton & Acrivos (1987*a*).

In the case of very dilute suspensions, the experimental apparatus lacked sufficient sensitivity to determine accurately the magnitude of the apparent slip. This prevented quantitative validation of Almog & Brenner's (1998) theoretical predictions, although the observed trends were in the right direction. In lieu of this confirmation, a boundary-element (BEM) simulation scheme involving numerical calculations of particle interactions in Stokes flows was used to model the fluid response to a sub-merged ball spinning in proximity to like-size neutrally buoyant spheres. These computational simulations displayed the same qualitative trends as did the experiments at higher concentrations, while matching the theoretical predictions of Almog & Brenner (1998) reasonably well at low concentrations.

The following section describes the physical properties of the suspensions employed, as well as the experimental apparatus and protocols. Analysis of the resulting measurements is reported in the subsequent section. Following this, we present the results of the BEM computations. Finally, our results are summarized and compared with existing theory (Almog & Brenner 1998) where appropriate.

2. Experiments

2.1. *Suspensions*

Monodisperse suspensions consisting of polymethyl methacrylate (PMMA) spheres uniformly dispersed in a highly viscous Newtonian liquid were created using three

different particle sizes. Two of these three classes of particles consisted of individually ground spheres of respective radii $a_2 = 1.59$ and 3.18 mm (Clifton Plastics Company), possessing published tolerances of ± 0.05 mm diameter and ± 0.025 mm sphericity. The third type of particle consisted of Diakon MG102 (ICI-United Kingdom) spheres sieved to yield an estimated mean radius of 0.327 ± 0.016 mm. The displayed tolerance is simply the range of sizes allowed between the sieve on which the particles were collected and that lying immediately above it.

The physical properties of each of the two suspending liquids employed in the experiments were established as follows: a Cannon-Fenske viscometer and Mettler/ PAAR DMA45 calculating digital density meter were, respectively, used to determine the liquid's kinematic viscosity and density. The operating temperature was adjusted until no observable sedimentation or flotation of the suspension as a whole occurred over a period of several days. The first mixture consisted of 36 wt % UCON-oil H-90 000, a polyalkylene glycol (Union Carbide Corporation), 14 wt % Triton X-100, an alkylaryl polyether alcohol (J. T. Baker), and 50 wt % 1,1,2,2-tetrabromoethane (Eastman Kodak). A small quantity (1 % of the weight of tetrabromoethane) of Tinuvin 328 (Ciba Geigy), an inhibitor, was added to the mixture to prevent breakdown and discoloration of the tetrabromoethane by ultraviolet radiation or dissolved iron. This mixture possessed a viscosity of 5.2 Pa s and a density that matched that of the 3.18 mm radius spheres at 19 °C. The second liquid used consisted of a mixture of 90 wt % UCON oil H-90 000 and 10 wt % 1,1,2,2 tetrabromoethane. The density of this mixture matched that of the 0.327 mm radius spheres at 25 °C as well as that of the 1.59 mm radius spheres at 17 °C. The respective viscosities of the mixture at these two temperatures were 4.1 and 6.5 Pa s. The large particles and choice of viscous fluids dictated that neither Brownian motion nor interparticle colloidal forces would affect the suspension behaviour.

The suspensions studied ranged in volume fraction varying from $c = 0.25$ to 0.50. Each suspension was prepared by individually weighing the desired fractions of particulate and fluid phases, and subsequently adding the spheres to the suspending liquid. Weighing was performed using a Mettler PM34 balance, accurate to ± 0.01 g. The suspensions were vigorously stirred by hand and allowed to de-gas prior to initiating each experimental procedure.

2.2. *Experimental apparatus*

Figure 1 depicts the spinning-ball viscometer apparatus. Fluid or suspension contained within the cylinder (inner radius $R_0 = 73.0$ mm) was rotated at a given rate by mounting the cylinder on a turntable. The ball was suspended along the cylinder axis by a thin rigid rod attached to a calibrated torsion wire, the latter being affixed to a mirror. The other end of the torsion wire was connected to an absolute encoder (Gurley 16 bit) mounted on the shaft of a servomotor (Reliance Electric model E586) so that the position of the upper mount of the torsion wire was always known accurately. Angular displacement of the ball resulted in a comparable rotation of the mirror. A Spectra-Physics Model 133 Helium–Neon Laser created a light beam that was, in turn, reflected from the suspended mirror to a laser-detector position sensor (United Detector Technology). The laser detector, which generates a voltage signal corresponding to the torsion wire displacement, was calibrated prior to each experiment using the absolute encoder as the reference. If the ball rotation caused the light beam to move off the detector, the servomotor served to bring the beam back to the detector. The angle through which the torsion wire was twisted by the action of the hydrodynamic torque on the sphere was then determined from the sum
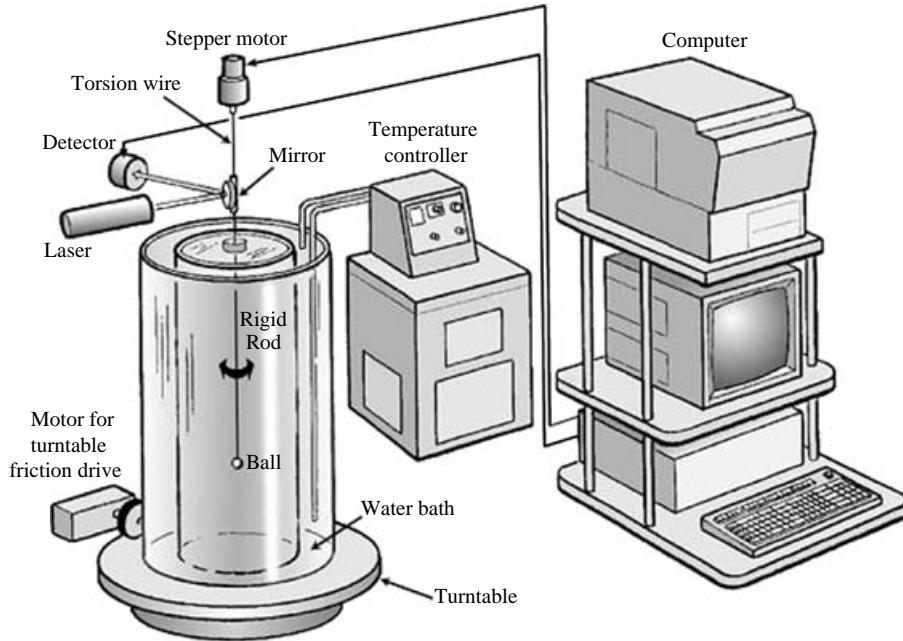
FIGURE 1. Sketch of the experimental apparatus.

of the angle measured from the encoder mounted on the servomotor and the angle computed from the laser-detector position sensor.

The turntable was driven with a Kollmorgen Motion Technologies PMI gear-reduced servomotor (9FGHDT/50:1) through a rubber friction drive wheel. A Kollmorgen KXA-48-8-16/PS/AUX servo amplifier was used together with the integral servomotor tachometer for closed-loop velocity feedback, so as to maintain a stable rotational velocity. Periodic recalibration of the tachometer voltage was performed using a magnetic sensor to count revolutions during a specified time interval. Also recorded was the tachometer voltage during each experiment, used to determine the instantaneous rotation rate Ω at each data acquisition time. Data acquisition was performed at a rate that ranged from five recordings per second for short-duration experiments (under 20 revolutions) to 20 recordings per minute for longer experiments (hundreds of revolutions).

As the suspending liquid properties depended strongly on temperature, experiments were performed in a controlled temperature environment. A constant-temperature circulator (Lauda Company, Brinkman Instruments), capable of maintaining a pre-set temperature to within $\pm 0.02\,^{\circ}$C, circulated cooling water through the jacket surrounding the suspension-containing vessel. The entire cylinder was insulated, including the top. (A small hole drilled in the top cover allowed the rod to rotate unimpeded.) Before and after each experiment, temperature measurements within the suspension were effected using an RTD probe accurate to $0.01\,^{\circ}$C. Capillary viscometer measurements, performed on the pure solvent over the narrow range of operating temperatures employed, provided the requisite viscosity data, μ_0, to correct for small temperature fluctuations as well as to estimate the accuracy of the spinning-ball viscometer measurements.

Four brass spinning balls were used, possessing respective radii a_1 of 3.18, 6.35, 9.53 and 12.7 mm. Permanently attached to the periphery of each ball was a brass rod of

radius $b = 0.57$ mm. During an experiment, this rod was attached to either one of two torsion wires, whose diameters were 0.2 and 0.4 mm. The larger torsion wire was used with the two larger balls and the smaller one with the two smaller balls. Each torsion wire was calibrated by measuring its period of free harmonic rotary oscillation with disks possessing known moments of inertia attached to the wire (Kunesh 1971).

Each experiment was performed in either one of two available modes – automatic or manual. In the automatic mode, used to record long-time data without an operator being present, a Kollmorgen KXA-48-8-16/PS/AUX servo amplifier was used for closed-loop control to keep the laser spot centred on the laser detector. The system could handle large angular displacements, and was, in fact, most stable when using the largest spinning ball (which resulted in an adequately large deflection of the torsion wire, accompanied by appropriate damping of any oscillations). However, in the automatic mode, fluctuations in the measured angle owing to the feedback control could not be absolutely separated from natural variations in twist angle arising from the temporally changing hydrodynamic interactions between the spinning ball and the suspended spheres immediately surrounding it. Accordingly, the system was operated in the manual mode to obtain most of the data reported here. In this mode the operator had to visually ensure that the laser spot remained focused on the detector.

2.3. *Calculation of the torques*

As the suspensions were relatively expensive, available resources were insufficient to create an apparatus large enough to accommodate a very large ball, which would have rendered negligible the additional torque created by the support rod in comparison with that created by the ball itself (as was, in fact, done by Kunesh 1971). Instead, we assumed the total torque recorded by the torsion wire to consist of the sum, L_t, of the respective torques, L and L_r, on the ball and supporting rod (Lamb 1932), each in isolation from the other:

$$L_t = L + L_r = 8\pi\mu_s a_1^3 \Omega + 4\pi\mu_s h b^2 \Omega, \tag{2}$$

with h the depth of submersion of the rod below the free surface of the liquid. Because of the linear response of the torsion wire, this torque was proportional to the angle θ through which the torsion wire was twisted, with the proportionality coefficient k appearing in the 'Hookean' relation $L_t = k\theta$ previously determined by calibration. Thus, in the absence of wall effects, the apparent viscosity μ_s of the suspension could be determined from the relation

$$\mu_s = \frac{k\theta}{4\pi\Omega\left(2a_1^3 + hb^2\right)}. \tag{3}$$

For a Newtonian fluid, Brenner (1964) showed that first-order boundary effects upon the torque experienced by a concentrically-positioned rotating sphere in a circular cylinder, arising respectively from the presence of the containing cylinder wall (radius R_0), cylinder bottom, and free surface are respectively of orders $(a_1/R_0)^3$ and $(a_1/b)^3$, where b is the distance of the sphere centre from the planar bottom or free surface. These wall effects, though already small, in relation to the torque being measured, were further minimized by positioning the sphere at the unique point (Brenner 1964) where the increased resistance to rotation of the ball due to its proximity to the cylinder bottom and walls is exactly offset by the lessened resistance resulting from the presence of the free surface. In our device, the height of the liquid varied with the concentration of particles, from about 17 cm to about 50 cm, because we increased the concentration by adding particles to either the suspending fluid or an existing

suspension. Therefore, this unique point varied slightly from experiment to experiment, ranging between 3.4 cm and 3.7 cm below the liquid surface. Although the wall effects arising in a suspension may not necessarily be identical to those experienced in a homogeneous Newtonian liquid, especially when the ball size is comparable to that of the suspended particles or to the mean distance between them, previous experience with comparable falling-ball rheometry experiments in suspensions leads us to believe that the use of Newtonian wall-effect corrections represents a reasonable approximation (Mondy *et al.* 1986).

The rotational Reynolds number, $Re = \Omega a_1^2 \rho / \mu_s$, was always less than 0.1 under the conditions encountered in our experiments. As such, inertial deviations from creeping-flow wall effects (Mena, Levinson & Caswell 1972) were not of concern.

3. Experimental results

3.1. *Pure suspending Newtonian liquid viscosities*

Equation (2) was used to determine the viscosity μ_0 of the Newtonian suspending solvent. Viscosities measured in this way using the spinning-ball apparatus were compared with those measured with the capillary viscometer at two nominal temperatures (20 and 25 °C) and at five nominal rotation rates (2, 5, 10, 15 and 18 r.p.m.). Torques produced under these conditions ranged from approximately 20 to 3200 g cm^2 s^{-2}. The approximation of adding together the separate torque contributions from the ball and the rod appears to be accurate even for our smallest ball, as shown in figure 2. The latter shows the torque measured in the Newtonian solvent versus the result of (2) calculated with the viscosity of the fluid determined by capillary measurements. Note that no wall-effect corrections are included in figure 2, and that the unique point serving to minimize wall effects in these experiments is situated at a depth of less than 3.7 cm.

Twenty-five tests spanning the above range of temperatures and rotation rates were performed with the 12.7 mm radius ball (figure 2*a*). The viscosity measured with the spinning-ball apparatus never differed by more than 6 % from that measured with the capillary viscometer, most differences being under 3 %. The largest deviations occurred with deepest submersion of the spinning ball. In actual experiments with suspensions, no more than 3.7 cm of rod extended below the surface of the liquid. Agreement between the capillary and spinning-ball viscosities was also within 5 %, with the other spinning balls situated at a depth of less than 3.7 cm. Results for the smallest spinning ball are shown in figure 2(*b*).

3.2. *Long-time suspension viscosity behaviour*

It is well documented (Leighton & Acrivos 1987*a*; Abbott *et al.* 1991; Chow, Sinton & Iwamiya 1994) that an initially homogeneous neutrally buoyant suspension of particles can become spatially inhomogeneous when subjected to slow flow in non-uniform shear fields. The spinning-ball apparatus creates just such an inhomogeneous flow field, leading to the expectation that the particles will, over time, migrate away from the high shear-rate region that exists in proximity to the rotating ball. This phenomenon would, in turn, be expected to lead to a reduction in torque over time, as observed with other rotational rheometers (Gadala-Maria & Acrivos 1980; Chow *et al.* 1994). Our initial suspension experiments were therefore designed to establish the time scale on which this migration phenomenon would affect the measured torque. Measurements of apparent slip could and would then be taken at shorter times, chosen to be significantly less than particle migration time scales. In such circumstances, the
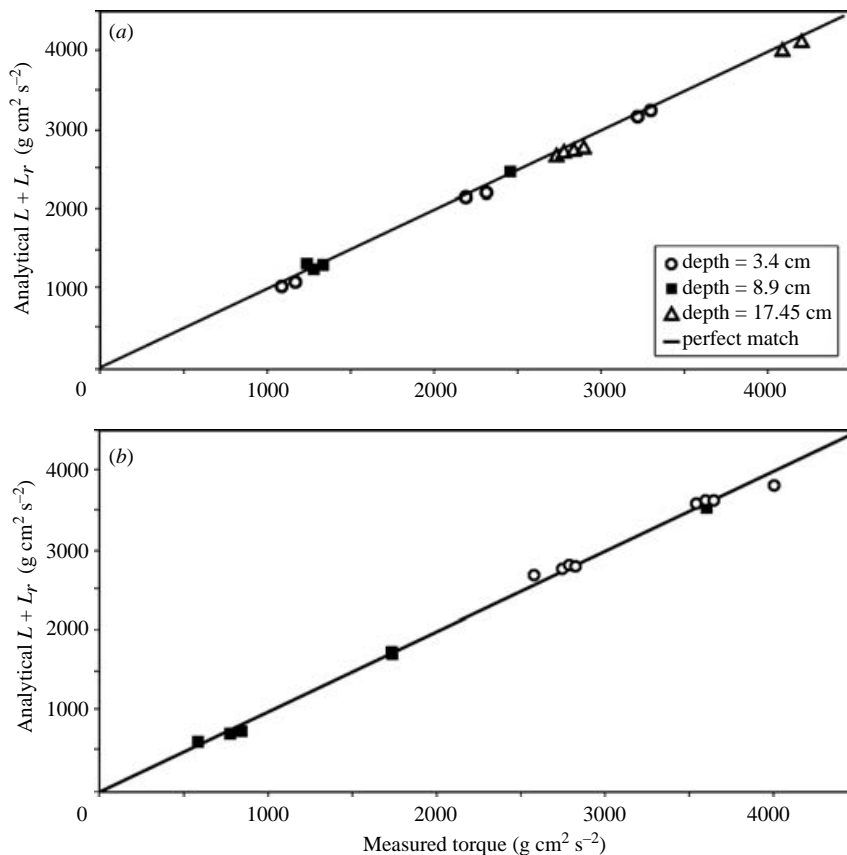
FIGURE 2. (*a*) The torque measured at various depths on a 12.7 mm radius ball suspended on a 0.57 mm radius rod at various rotational rates compared with the analytical approximation, equation (2); (*b*) The torque measured at two depths on a 3.18 mm radius ball suspended on a 0.57 mm radius rod at various rotational rates compared with the analytical approximation, equation (2).

initial configuration of particles would be expected to approximate the homogeneous well-mixed distribution that presumably existed prior to the start of the experiment.

Figure 3 is a plot of the relative suspension viscosity, $\mu_r = \mu_s/\mu_0$, namely, the viscosity μ_s of a $c = 0.50$ suspension of 3.18 mm radius spheres measured in the spinning-ball apparatus, divided by the solvent viscosity measured in the capillary viscometer at the same temperature. The suspension viscosity μ_0 was recorded with a 12.7 mm radius spinning ball at a rate of 5 measurements per second for the first 20 revolutions, subsequently reduced to a rate of 20 measurements per minute thereafter. Also shown is the corresponding ratio for the pure solvent. In the suspension, the torque signal fluctuated far more in magnitude than in the corresponding suspension-free solvent case, the enhancement presumably arising from interactions between the suspended particles and the spinning ball. Furthermore, a significant reduction in torque with cumulative number of revolutions is apparent, as was to be expected as a consequence of ongoing particle migration away from the spinning ball. No comparable reduction occurred in the pure solvent viscosity as measured in the spinning-ball apparatus. In addition to the expected reduction in torque at relatively
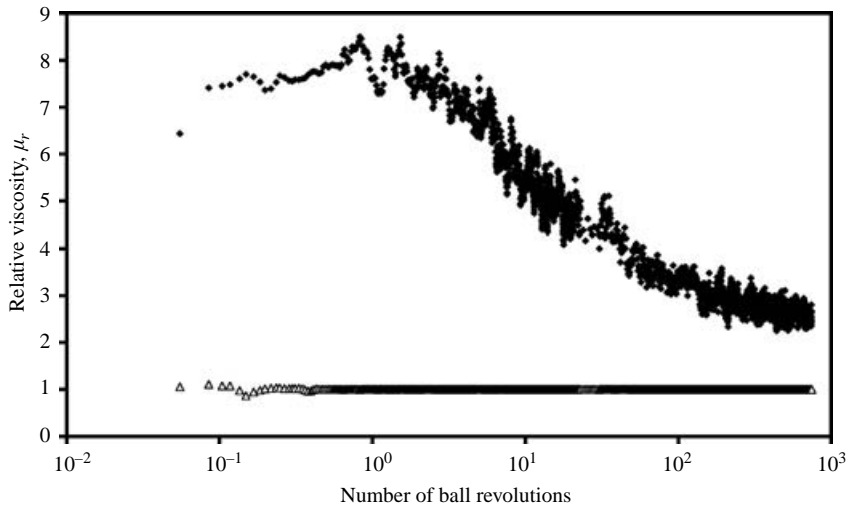
FIGURE 3. Spinning ball viscosity of a suspension with $c = 0.50$ (diamonds) and the pure solvent (triangles), both normalized by the capillary-measured viscosity of the pure solvent.

long times, there was an initial increase in torque upon start-up, as discussed in the next subsection.

Because the torque at any instant of time is a function of the instantaneous local configuration of the suspended spheres proximate to the spinning ball, we repeated the measurements for each suspension and each ball size several times, vigorously stirring the suspension prior to each experiment in an attempt to achieve an initially spatially homogeneous distribution of particles. Based upon observations of comparable falling-ball experiments (Mondy *et al.* 1986; Abbott *et al.* 1998), we expected that this procedure, involving the vigorous mixing of the suspension before each experiment and the averaging of several measurements performed during the early stages of different experiments (i.e. prior to the onset of significant lateral migration), would provide a meaningful measure of the couple experienced by a ball in a suspension of approximately randomly distributed spheres at the specified (mean) particle concentration. (The hand-mixing technique also has been shown to result in a seemingly random distribution of orientations of non-spherical suspended particles, Mondy *et al.* 1990.)

Figure 4 is a plot of the relative viscosity for five experiments performed with the 12.7 mm radius spinning ball in a suspension of 3.18 mm radius spheres at $c = 0.50$. Each point represents an average over three to ten revolutions for any one experimental protocol. Two observations pertaining to these data are particularly noteworthy. (i) Despite these experiments being performed at essentially three significantly different rotation rates, nominally 5, 10 and 15 r.p.m., the data collapsed onto a single curve. This observation is consistent with the diminution in suspension viscosity over time being caused by shear-induced migration of the particles (Leighton & Acrivos 1987*b*; Phillips *et al.* 1992), where the particle migration is dependent upon the absolute strain, but not the strain rate. (ii) The initial viscosity measured in any one experiment differed from that measured in other 'equivalent' experiments by as much as 15 to 20 %. This variation between experiments is much larger than was observed with the pure suspending solvent under the same conditions, and presumably reflects differences caused by variations in the microscale distribution of suspended particles
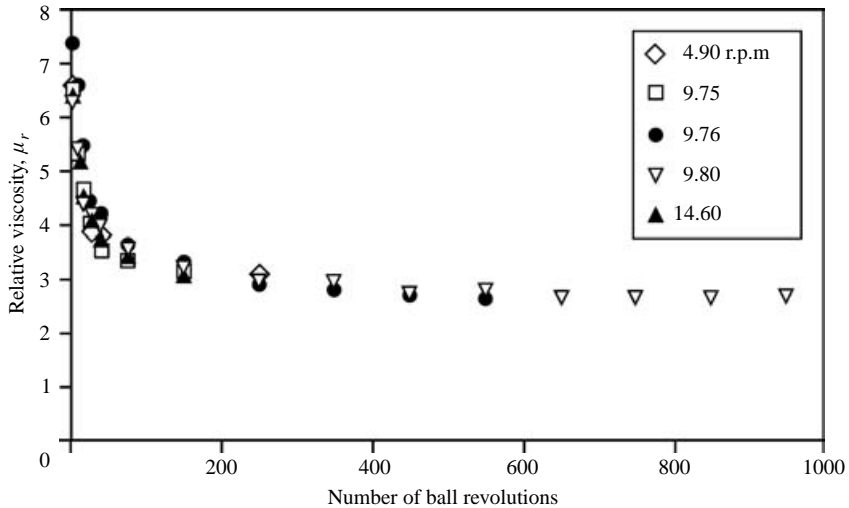
FIGURE 4. Spinning ball viscosity at various rates of rotation for a suspension of 3.2 mm radius spheres ($c = 0.50$) as measured using a 12.7 mm radius spinning ball.

in the neighbourhood of the spinning ball. Because of the relatively rapid initial apparent viscosity diminution with increasing number of revolutions manifested in figures 3 and 4, the phrase 'early time' in the subsequent discussion is defined to be that occurring before four ball revolutions.

3.3. *Short-time suspension viscosity behaviour*

As seen in figure 3, there occurs an initial increase in the torque measured in a concentrated suspension during the first ball revolution. Because we see no initial rise in the torque in the suspending fluid, this increase in the torque measured in a suspension is not thought to be caused by the finite time required for the system to respond to the imposed steady rotation rate begun from rest. Rather, it appears more likely to be caused by microstructural changes in the configuration of particles created in the concentrated suspensions by the flow field, or by a longer-than-expected transient start-up period due to minute inertial effects in the two-phase fluid. As will be discussed later, using BEM simulations, we tested the hypothesis that the couple experienced by a ball after one revolution in a suspension could be considered as identical to that in a suspension of randomly distributed particles. In these numerical simulations, we compared the initial torque for a 'snapshot' of randomly distributed spheres to the torque observed after several revolutions of the spinning ball. We found that the couple increases slightly during the first few revolutions in the dynamic simulations, providing further evidence that the initial increase is caused by microstructural changes in the configuration of particles. Because the measured viscosity seemed to be fairly constant between one and four revolutions in the experiments, it is this viscosity that we will take to be the 'early time' value in the following narrative.

The early-time relative viscosity μ_r (measured between 1 and 4 revolutions of the 12.7 mm radius ball) of the 0.327 mm radius particle suspensions was found to be close to the comparable suspension viscosity values gleaned from other types of rheometric measurements, as shown in figure 5. Here, we are comparing our results with data on suspensions of fairly uniform particles taken in shear and capillary rheometers, as collated by Thomas (1965). The point shown for $c = 0.25$ represents an average of three
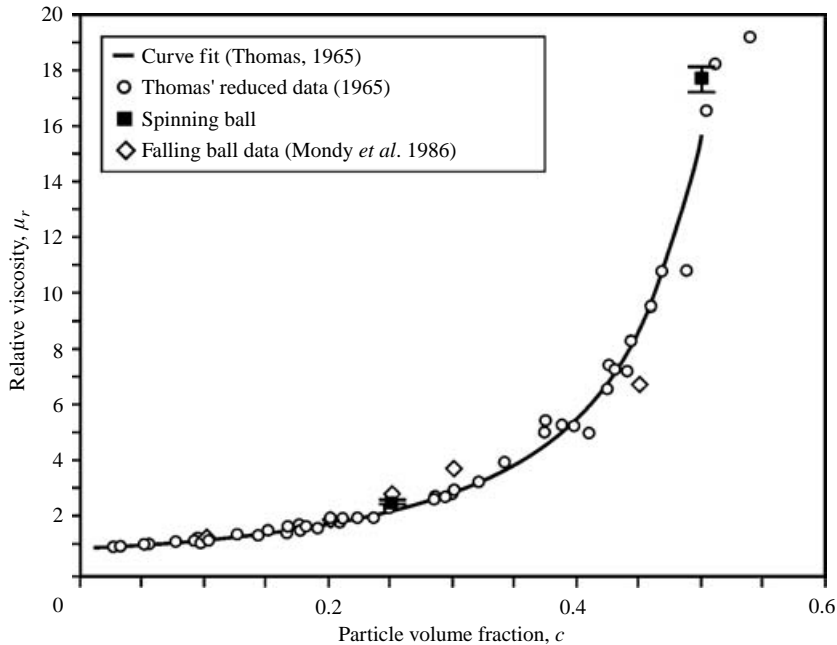
FIGURE 5. Spinning ball relative viscosity (measured with a 12.7 mm radius ball for suspensions of 0.327 mm radius spheres) compared with rheometric literature values (Thomas 1965).

experiments, each experiment representing an average of measurements performed after more than one, but less than four revolutions. The point for $c = 0.50$ represents the average of six such experiments. Error bars denote the 95 % confidence limits on the measurements based upon a Student's t-test conducted among the separate experiments.

As the suspended particle size increased relative to that of the spinning ball, the early-time (measured between one and four revolutions) apparent relative suspension viscosity $\mu_r = \mu_s / \mu_0$ measured with the spinning-ball apparatus decreased dramatically. Figure 6 illustrates this phenomenon for the $c = 0.25$, 0.40 and 0.50 suspensions. As discussed in §1, this decrease in apparent viscosity can be interpreted as an apparent slip on the surface of the spinning ball. Data for several spinning ball sizes at several different suspension concentrations are included. For clarity, a representative Student's t-test confidence limit is shown for one point only. Within estimated experimental error, at the same concentration, no difference exists among those points characterized by the same a_2/a_1 ratio, but differing in their individual a_1 and a_2 values.

4. Boundary-element simulations

In order to bridge the gap between the experimental evidence of slip in concentrated suspensions and the dilute suspension theory of Almog & Brenner (1998), boundary-element simulations of the spinning ball viscometer were performed. Three-dimensional results for both instantaneous torque calculations from randomly generated initial configurations and transient simulations were obtained. As the boundary-element formulation has been documented and extensively benchmarked
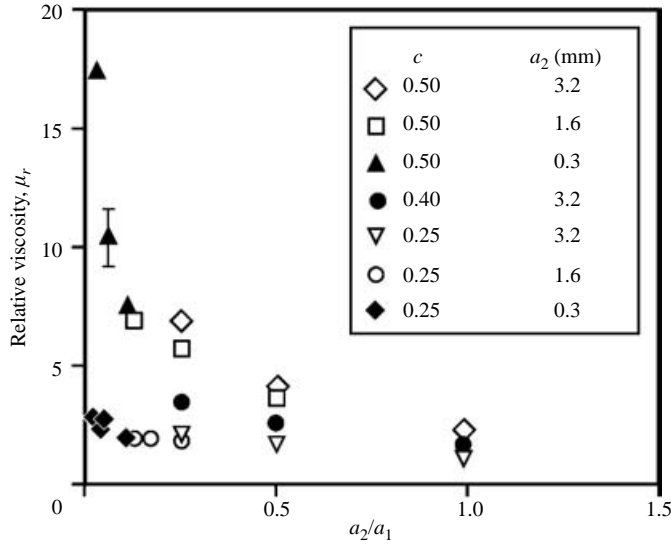
FIGURE 6. Spinning ball relative viscosity measurements for seven suspensions as a function of the ratio of suspended-sphere/spinning-ball radius and for varying concentrations.

elsewhere (see e.g. Dingman *et al.* 1992; Ingber & Mondy 1993), only a brief overview of the scheme is outlined here for completeness.

The velocity field for Stokes flow can be represented at an arbitrary field point y in a domain possessing a boundary Γ by the boundary-integral equation,

$$c_{ij}(y)u_j(y) + \int_{\Gamma} q^*_{kji}(y, x)u_k(x)n_j(x)\,d\Gamma = -\int_{\Gamma} u^*_{ik}(y, x)f_k(x)\,d\Gamma, \qquad (4)$$

where u_k and f_k are the respective components of the velocity and traction fields on the boundary Γ, n_j is the component of the unit outward-normal vector on the boundary, and u^*_{ik} and q^*_{kji} are, respectively, the fundamental singular Stokes velocity and stress fields:

$$u^*_{ik} = \frac{1}{8\pi}\left(\frac{\delta_{ik}}{r} + \frac{(x_i - y_i)(x_k - y_k)}{r^3}\right), \qquad (5)$$

$$q^*_{ijk}(x, y) = \frac{3}{4\pi}\frac{(x_i - y_i)(x_j - y_j)(x_k - y_k)}{r^5}, \qquad (6)$$

Here, $r = |y - x|$ denotes the distance between points y and x, and δ_{ij} is the Kronecker delta. The coefficient c_{ij} appearing in (4) can be determined from the geometrical configuration of the system; however, for those field points lying on smooth portions of the boundary, $c_{ij} = \delta_{ij}/2$. For most problems, at each point in the domain, either the appropriate velocity or traction component is specified for each coordinate direction. The solution of the discretized boundary-integral equations provides a representation of the unknown boundary information. This is the case for: (i) the surface of the cylindrical container, where the velocity is set to zero; and (ii) the surface of the spinning ball, where the solvent velocity is prescribed by the ball's rotation rate. However, on the surfaces of the suspended spheres, neither the solvent velocity nor the solvent traction components are explicitly known *a priori*. In order to close the system of equations, the boundary integral equation is supplemented with both

kinematic and dynamic constraints specifying the force- and torque-free status of each of the suspended spheres.

The kinematic conditions specify that each suspended particle behaves as a rigid body on whose surface the solvent adheres. As such, these equations serve to relate the solvent velocity u_i at each point on a particle's surface to the particle's centroidal linear and angular velocities. These equations are thus written as

$$u_i = u_i^p + \varepsilon_{ijk}\Omega_j^p x_k, \tag{7}$$

where u_i and u_i^p are, respectively, the components of the solvent velocity vector at the surface of the particle and the particle velocity vector at the centre of the pth sphere. Here, Ω_j^p represents the angular velocity vector of the pth sphere, x_k is the displacement vector of a point lying on the suspended sphere surface relative to its centre, and ε_{ijk} is the alternating unit tensor.

The quasi-static dynamical equations governing the forces and torques acting on the suspended particles are consistent with the Stokes approximation, in the sense that particle accelerations are neglected. The resulting equations for the pth particle are

$$\int_{\Gamma_p} f_i \, \mathrm{d}\Gamma + F_i^p = 0, \tag{8}$$

$$\int_{\Gamma_p} \varepsilon_{ijk} x_j^p f_k \, \mathrm{d}\Gamma + T_i^p = 0, \tag{9}$$

in which F_i^p and T_i^p are, respectively, the external force and torque (the latter about the particle centre) exerted on the pth particle, and Γ_p denotes the surface of the pth particle. For the spinning-ball problem, it is assumed that the spheres comprising the suspension are freely suspended and neutrally buoyant, whence both F_i^p and T_i^p are set equal to zero. Together with (4) and (7)–(9), the resulting physical problem is well posed.

The boundary element chosen for this calculation is a superparametric element in which the boundary geometry is quadratically approximated, and functional approximations are taken to be constant within the elements. An adaptive quadrature technique is used, wherein the number of Gauss points within an element is a function of an integration severity number (Ingber & Mondy 1993). Essentially, the latter is a measure of some characteristic dimension of the element divided by the distance from the collocation node to the element. The larger the severity number, the larger the number of Gauss points used to evaluate the boundary integrals numerically.

Fully three-dimensional calculations were performed for both a dilute suspension ($c = 0.03$) and a moderately concentrated suspension ($c = 0.25$) using a range of size ratios a_2/a_1. The spinning ball was placed in the centre of a cylinder of (dimensionless) height 10 and diameter 10 which was filled with fluid of viscosity $\mu_0 = 1$. For each simulation, 220 spherical particles were placed in the viscometer domain using a random number generator. The sizes of both the particles and the spinning ball were chosen to achieve a given size ratio and particle concentration. For each case, the domain was meshed with 122 nodes per particle and 5762 on the surrounding cylinder. For the dilute simulations, the spinning ball was meshed with 122 nodes, whereas for the more concentrated cases, the spinning ball was meshed with 362 nodes (or 1522 nodes for the case with the largest spinning ball, $a_2/a_1 = 0.25$). Figure 7 shows a typical mesh with a random starting configuration.
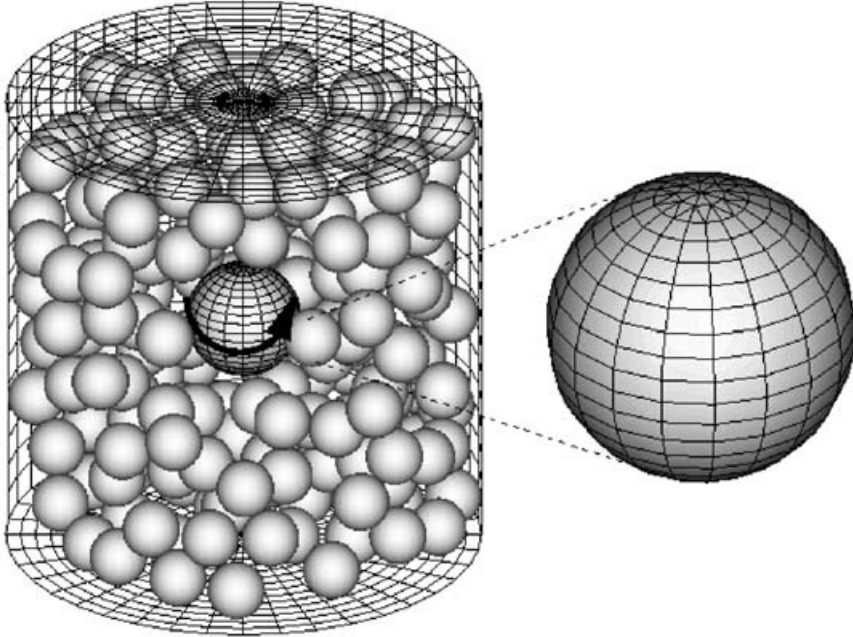
FIGURE 7. Typical grid of spinning ball in a cylinder filled with suspended balls. Here $a_2/a_1 = 0.5$ and $c = 0.25$. The particles in front of the spinning ball have been made transparent.

For each case, an initial Newtonian torque L_N was calculated by performing a simulation without particles being present. To calculate the suspension viscosity, two methods were used. For all cases, an instantaneous torque was calculated using the random initial configuration. Because the torque was observed to be highly dependent on the arrangement of the suspended particles, all results were ensemble averaged over many initial configurations (using ensembles of 10–60 configurations). Dynamic torque measurements were also determined by performing transient simulations starting from the random initial configuration. Since these systems are not ergodic, results from the transient simulations were also ensemble averaged. The calculated values of the torque are presented either in terms of the relative viscosity $\mu_r = \mu_s/\mu_0$ or as a dimensionless extra torque $\Delta L' = (L_s - L_N)/8\pi\mu_0 a_1^3 c\Omega$, where L_s is the suspension torque and Ω is the rotation rate of the spinning ball (which in all cases is 2π in non-dimensional units).

In order to characterize finite-size effects in the computational domains as well as mesh-resolution effects, Newtonian torque results are compared with (1) for a spinning ball in an infinite domain. These results are presented in figure 8 as a function of the radius of the spinning ball, where the torque has been non-dimensionalized by the analytical solution equation (1).

For the dilute-solution calculations, where the radius of the spinning ball tends to be small relative to the cylinder radius of 5, the Newtonian results are seen to be only slightly larger ($< 1\%$) than the analytical solution. However, even for a fairly large spinning ball radius of 1.2, the deviation from (1) is only 2%. This corresponds to a spinning ball radius which is twice the size of the suspended particle at a concentration $c = 0.25$ in the standard cylinder size (diameter $= 10$ and height $= 10$). Several test cases are also shown, keeping the spinning ball size constant and increasing ball resolution (to 1522 nodes), cylinder resolution (to 23 362 nodes), or cylinder height
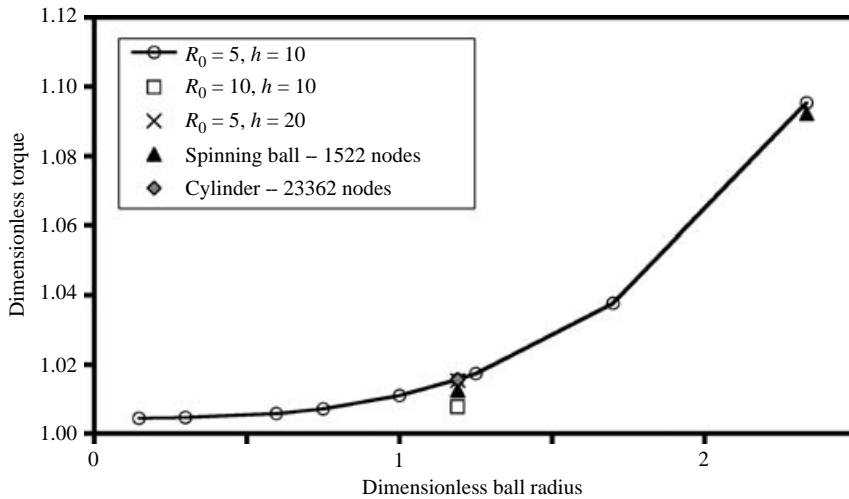
FIGURE 8. Comparison of the Newtonian torque with the analytical prediction. Standard resolution includes 122 nodes on each suspended particle, 362 nodes on the spinning ball, and 5762 nodes on the cylinder. Values for higher-resolution meshes are also shown.

or radius. Some tests were also performed for a concentration of $c = 0.25$ with higher particle resolution (290 nodes per particle), but the latter were found to have minimal effect on the calculated torque. The most important limiting factor is the finite size of the container (specifically its radius) that in turn is limited by the number of particles we can simulate.

Instantaneous dimensionless couples calculated from random initial configurations for a dilute concentration of 0.03 are shown in figure 9 for two ensemble sizes, 10 and 60 initial particle configurations. Both results compare favourably with Almog & Brenner's (1998) dilute suspension theory. Though there is clearly more scatter with the smaller ensemble size, the ensemble size of 10 is believed to be large enough to capture the configuration dependence of the system. The simulations also appear to consistently underpredict the analytical theory. In short transient boundary-element simulations for 8 revolutions of the spinning ball, there was no variation in the torque ($< 0.5 \%$). Thus, for dilute solutions, the particle structure appears to be unaffected by flow, whence the initial randomly generated configurations adequately describe the system microstructure.

For a moderately concentrated suspension ($c = 0.25$), suspension viscosities calculated from ensemble averages of 10 random initial configurations are compared in figure 10 with experimentally measured relative suspension viscosities. The boundary-element simulations are again seen to underpredict the expected viscosity of the suspension. To test the possible influence of the use of a random particle configuration upon the torque measurements, transient calculations were performed for several ratios of ball to suspended-particle size. In other flows of concentrated suspensions, flow-induced structure formation has been observed (Gadala-Maria & Acrivos 1980; Parsi & Gadala-Maria 1987; Morris & Brady 1997). By performing dynamic calculations, the possible effects of flow-induced structure can be included in the comparison with experiment. For each of the 10 initial configurations, the flow is simulated for 5–10 revolutions of the spinning ball, and the transient torques ensemble averaged. Figure 11 shows the combined transient torque data for 10 configurations
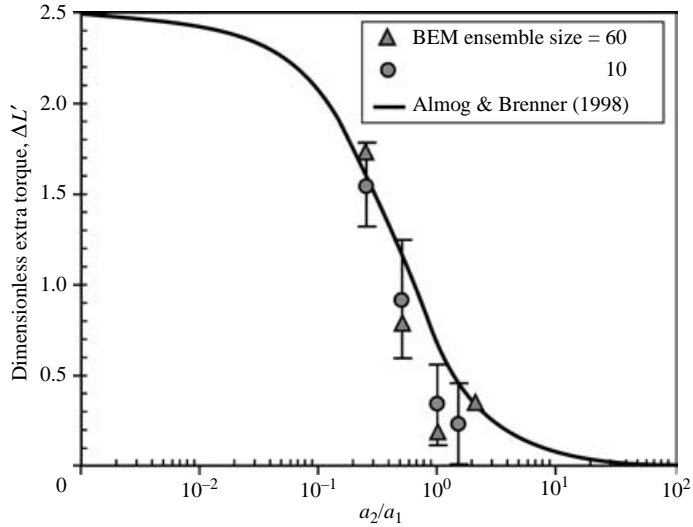
FIGURE 9. Comparison of boundary-element simulations to Almog & Brenner's (1998) dilute theory for $c = 0.03$.
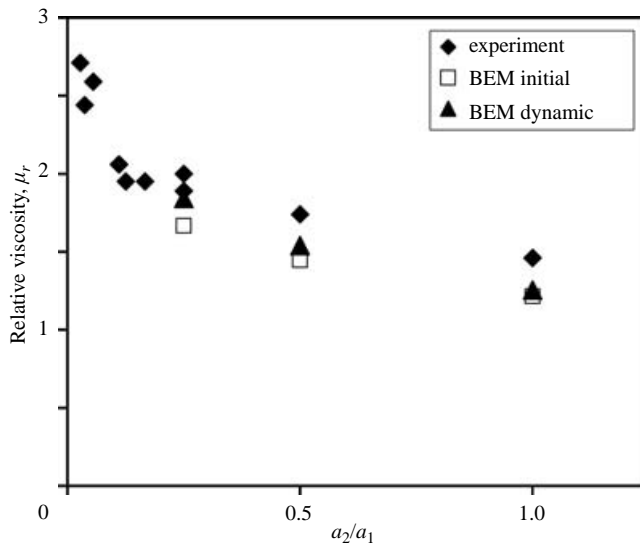

FIGURE 10. Comparison of relative viscosity from experiment and boundary-element simulation for $c = 0.25$.

with $a_2/a_1 = 0.25$, as well as the resulting averaged torque. For other cases where the spinning ball is larger than the suspended particles, the torque is also seen to increase when the flow is started, whereas for $a_2/a_1 > 1$, the change in the torque is small ($< 0.5\%$ for $a_2/a_1 = 2$). After several revolutions, the averaged torque stops increasing and reaches an approximate plateau. The value is then averaged over a ball revolution and used to calculate the dynamic relative viscosity shown in figure 10. This plateau region is by no means a steady-state viscosity, but rather is thought to represent a more accurate comparison with the averaged initial torque measured in
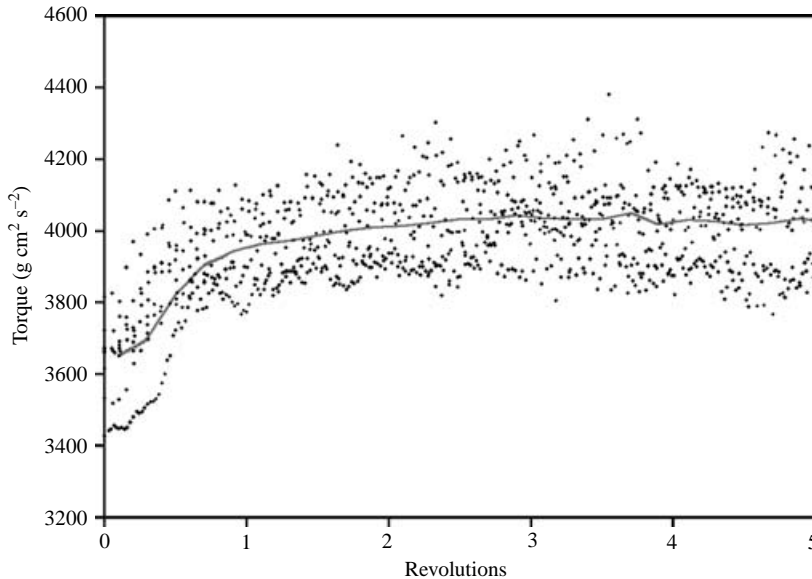
FIGURE 11. Averaged torque (line) compared with transient torque for 10 different initial configurations (symbols).

the experiments. The simulations took longer to reach this plateau than did the actual experiments (about 2 or 3 revolutions). For longer times, the calculated torque is seen to decrease in the same manner as observed experimentally (figure 12); however, steady state is achieved much faster. We speculate that that is because of the relatively small system size in the simulations.

5. Summary and conclusions

The torque on a ball rotating at small Reynolds numbers in an otherwise quiescent suspension of comparably-sized neutrally buoyant spheres was measured experimentally for different concentrations of suspended particles, ball angular velocities and ratios of spinning ball to suspended-sphere sizes. This 'spinning-ball viscometer' was initially tested by using (2) to confirm the known viscosity of the homogeneous Newtonian interstitial suspending liquid. The outcome of the spinning-ball viscosity measurements performed on the pure Newtonian solvent differed by only a few per cent from the comparable viscosities measured independently with a capillary viscometer. This suggests that the hypothesized linear additivity of the respective torques on the ball and rod, each rotating in isolation from the other, did not result in significant errors.

During the suspension experiments the torque on the spinning ball initially increased, then decreased with increasing number of revolutions, ultimately approaching an asymptote. This phenomenon did not occur during the comparable homogeneous Newtonian liquid experiments, where the torque remained independent of the number of ball revolutions. The suspensions were initially well stirred. We speculate that the initial torque increase is caused by a change in the suspension's microstructure due to the resulting flow at short times. Subsequently, the torque decreased as the cumulative number of revolutions of the ball increased, presumably as the suspended particles migrated away from the high shear-rate region existing in
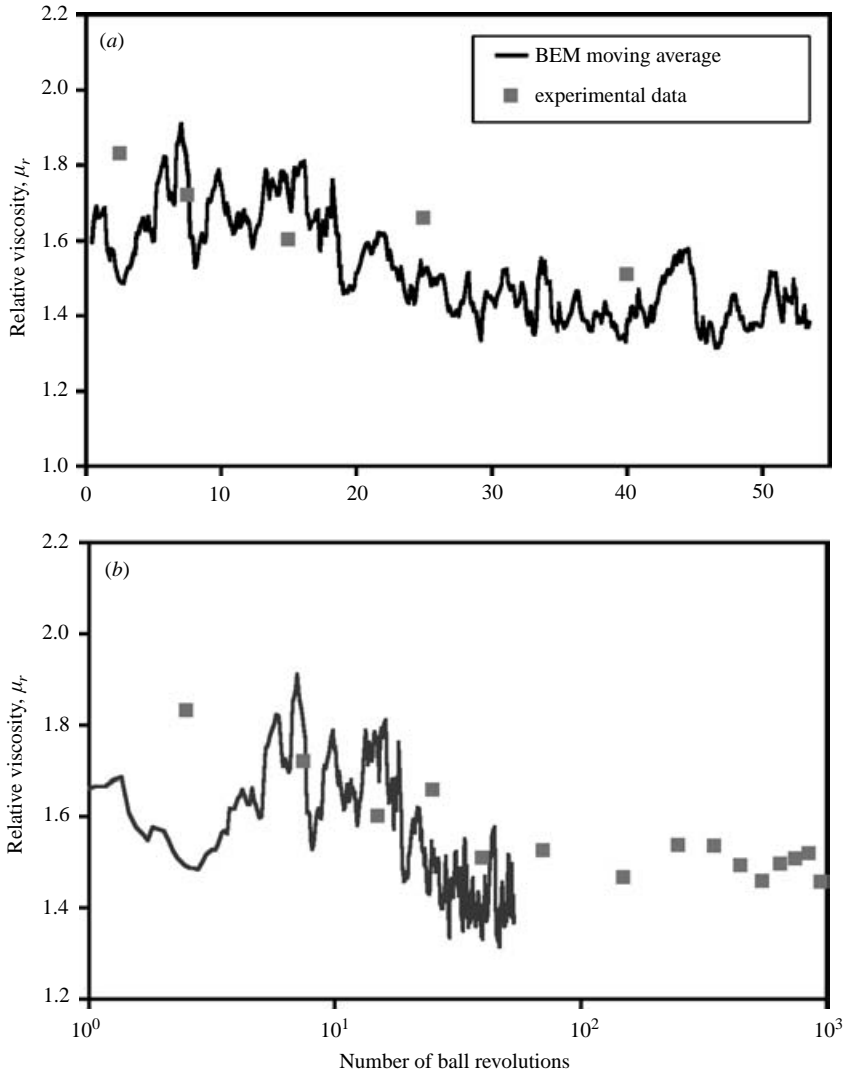
FIGURE 12. Long-time three-dimensional transient simulation results compared with experiments. (*a*) is an expanded view of (*b*).

proximity to the spinning ball. All other things being equal except angular velocity, this temporal torque diminution depended only upon the total number of ball rotations, but not upon the characteristic shear rate. This is consistent with other low-Reynolds-number shear-induced migration phenomena (Leighton & Acrivos 1987*b*; Phillips *et al.* 1992). The instantaneously measured torque on the spinning ball also fluctuated only in the case of the suspensions, but not in the homogeneous suspending-fluid case, leading to the speculation that the observed fluctuation phenomenon is caused by time-dependent hydrodynamic interactions of the spinning ball with the suspended particles arising from temporal changes in the local suspended particle configuration and, hence, local suspension 'concentration' *c*. These observations are consistent with the results of our dynamic boundary-element calculations for a ball spinning in a suspension of similar spheres.

Use of (2) to interpret the torque measured initially in a presumably homogeneous suspension, served to define the apparent viscosity of the suspension based on the supposition that the latter could initially be regarded as a homogeneous Newtonian-like continuum prior to the development of inhomogeneities arising from shear-induced particle migration, and that no slip prevailed at the surface of the spinning ball. This short-time (spinning-ball) apparent viscosity agreed fairly well with earlier experiments (see the summary by Abbott *et al.* 1998) using falling-ball viscometry for similarly constituted suspensions (i.e. possessing the same volume fraction c, same suspended particle size a_2, etc.) as well as with other published values for measurements in shear and capillary viscometers (Thomas 1965). For a given suspension, as the ratio a_2/a_1 became larger the apparent spinning-ball viscosity decreased dramatically, thereby exhibiting an apparent surface 'slip'. This ball-size phenomenon was anticipated in this range of a_2/a_1 values based upon theoretical predictions by Almog & Brenner (1998), albeit for dilute suspensions. The apparent slip became more pronounced with increasing suspension concentration c.

Fully three-dimensional boundary-element method (BEM) simulations of the interstitial Stokes flow arising from a ball spinning in a dilute suspension of neutrally buoyant spheres were performed. The boundary conditions imposed on each particle included no-slip between the interstitial fluid and the particle's surface. The calculated torque obtained during these particle-level simulations was consistent with that obtained by approximating the suspension as a hypothetical homogeneous single-phase fluid while imposing a partial slip boundary condition at the spinning ball surface. Calculations for a $c = 0.03$ suspension compared well with the theoretical predictions of Almog & Brenner (1998), confirming that such slip becomes more pronounced as the ratio a_2/a_1 increases.

BEM simulations performed at moderately high concentrations of suspended spheres ($c = 0.25$) agreed with our experimental observations. These simulations displayed fluctuations in the instantaneous configuration-specific torque on the spinning ball, as well as manifesting an initial short-time increase in torque followed by an overall decrease in torque with increasing number of revolutions – both phenomena being qualitatively in agreement with our experiments. Inasmuch as the numerical simulations assume Stokes flow and an infinite Péclet number, the initial increase in torque observed in the simulations can only be attributed to microstructural changes occurring in the local particle distribution caused by the flow.

Like its falling-ball counterpart, the spinning-ball rheometer provides a unique tool for statistically probing discrete non-continuum aspects of suspension behaviour. The ability to do so arises from the fact the 'tracer' is comparable in size to the suspended particles and/or to the mean distance separating them. This attribute, coupled with the fact that the suspension is quiescent except for the fluid motion generated by the probe itself, results in the tracer responding to microscale fluctuations in local particle concentration occurring in its immediate environment. In the falling-ball case, such fluctuations are manifested as a Fickian dispersion phenomenon (Abbott *et al.* 1998). A comparable dispersion theory, globally quantifying the statistics of the fluctuations in the corresponding spinning-ball case, has yet to be developed.

Massachusetts Institute of Technology by the US Department of Energy, Division of Engineering and Geosciences, Office of Basic Energy Sciences.

REFERENCES

ABBOTT, J. R., GRAHAM, A. L., MONDY, L. A. & BRENNER, H. 1998 Dispersion of a ball settling through a quiescent neutrally buoyant suspension. *J. Fluid Mech.* **361**, 309–331.

ABBOTT, J. R., TETLOW, N., GRAHAM, A. L., ALTOBELLI, S. A., FUKUSHIMA, E. & STEPHENS, T. S. 1991 Experimental observations of particle migration in concentrated suspensions: Couette flow. *J. Rheol.* **35**, 773–795.

ALMOG, Y. & BRENNER, H. 1997 Non-continuum anomalies in the apparent viscosity experienced by a test sphere moving through an otherwise quiescent suspension. *Phys. Fluids* **9**, 16–22.

ALMOG, Y. & BRENNER, H. 1998 Apparent slip at the surface of a small rotating sphere in a dilute quiescent suspension. *Phys. Fluids* **10**, 750–752.

BEN-AMOTZ, D. & SCOTT, T. W. 1987 Microscopic frictional forces on molecular motion in liquids. Picosecond rotational diffusion in alkanes and alcohols. *J. Chem. Phys.* **87**, 3739–3748.

BRENNER, H. 1964 Slow viscous rotation of an axisymmetric body within a circular cylinder of finite length. *Appl. Sci. Res.* A. **13**, 81–120.

BRENNER, H. 1972 Suspension rheology in the presence of rotary Brownian motion and external couples: elongational flow of dilute suspensions. *Chem. Engng Sci.* **27**, 1069–1107.

CHOW, A. W., SINTON, S. W. & IWAMIYA, J. H. 1994 Shear-induced particle migration in Couette and parallel-plate viscometers: NMR imaging and stress measurements. *Phys. Fluids* **6**, 2561–2576.

DEBYE, P. 1929. *Polar Molecules*. Dover.

DINGMAN, S., INGBER, M. S., MONDY, L. A., ABBOTT, J. R. & BRENNER, H. 1992 Particle tracking in three-dimensional Stokes flow. *J. Rheol.* **36**, 413–440.

EINSTEIN, A. 1906 Eine neue Bestimmung der Moleküldimensionen *Annln Phys.* **19**, 289–306.

EINSTEIN, A. 1911 Berichtigung zu meiner Arbeit: 'Eine neue Bestimmung der moleküldimensionen'. *Annln Phys.* **34**, 591–592.

EINSTEIN, A. 1956 *Investigations on the Theory of the Brownian Movement*. Dover.

GADALA-MARIA, F. & ACRIVOS, A. 1980 Shear-induced structure in a concentrated suspension of solid spheres. *J. Rheol.* **24**, 799–814.

HAPPEL, J. & BRENNER, H. 1986 *Low Reynolds Number Hydrodynamics*, 159–173. Martinus Nijhoff.

INGBER, M. S. & MONDY, L. A. 1993 Direct second-kind boundary integral formulation for Stokes flow problems. *Computational Mech.* **11**, 11–17.

KOENDERINK, G. H. 2003 Rotational and translational diffusion in colloidal mixtures. Universiteit Utrecht, PhD thesis.

KUNESH, J. G. 1971 Experiments on the hydrodynamic resistance of translating-rotating particles. Carnegie Mellon University, PhD thesis.

KUNESH, J. G., BRENNER, H., O'NEILL, M. E. & FALADE, A. 1985 Torque measurements on a stationary axially-positioned sphere partially and fully submerged beneath the free surface of a slowly rotating viscous fluid. *J. Fluid Mech.* **154**, 29–42.

LAMB, H. 1932 *Hydrodynamics*, 6th edn, p. 585. Cambridge University Press.

LEIGHTON, D. & ACRIVOS, A. 1987a Measurement of shear-induced self-diffusion in concentrated suspensions of spheres. *J. Fluid Mech.* **177**, 109–131.

LEIGHTON, D. & ACRIVOS, A. 1987b The shear-induced migration of particles in concentrated suspensions. *J. Fluid Mech.* **181**, 415–439.

MENA, B., LEVINSON, E. & CASWELL, B. 1972 Torque on a sphere inside a rotating cylinder. *Z. Angew. Math. Phys.* **23**, 173–181.

MILLIKEN, W. J., MONDY, L. A., GOTTLIEB, M., GRAHAM, A. L. & POWELL, R. L. 1989 The effect of the diameter of falling balls on the apparent viscosity of suspensions of spheres and rods. *PhysicoChem. Hydrodyn.* **11**, 341–355.

MONDY, L. A., GRAHAM, A. L. & JENSEN, J. L. 1986 Continuum approximations and particle interactions in concentrated suspensions. *J. Rheol.* **30**, 1031–1051.

MONDY, L. A., MORRISON, T. G., GRAHAM, A. L. & POWELL, R. L. 1990 Measurements of the viscosities of suspensions of oriented rods using falling ball rheometry. *Intl J. Multiphase Flow* **6**, 651–662.

Morris, J. F. & Brady, J. F. 1997 Microstructure of strongly sheared suspensions and its impact on rheology and diffusion. *J. Fluid Mech.* **348**, 103–139.

Parsi, F. & Gadala-Maria, F. 1987 Fore-and-aft asymmetry in a concentrated suspension of solid spheres. *J. Rheol.* **31**, 725–732.

Phillips, R. J., Armstrong, R. A., Brown, R. A., Graham, A. L. & Abbott, J. R. 1992 A constitutive equation for concentrated suspensions that accounts for shear-induced particle migration. *Phys. Fluids* **4**, 30–40.

Sluch, M. I., Somoza, M. M. & Berg, M. A. 2002 Friction on small objects and the breakdown of hydrodynamics in solution: rotation of anthracene in poly(isobutylene) from the small-molecule to polymer limits. *J. Phys. Chem.* B **106**, 7385–7397.

Stokes, G. G. 1851 On the effect of the internal friction of fluids on the motion of pendulums. *Proc. Camb. Phil. Soc.* **9**, 8–106.

Thomas, D. G. 1965 Transport characteristics of suspensions VIII: a note on the viscosity of Newtonian suspensions of uniform spherical particles. *J. Colloid Sci.* **20**, 267–277.